# EXPERIMENTAL AND ANALYTICAL STUDIES ON FLEXURAL BEHAVIOR OF POST-TENSIONED CONCRETE BEAM SPECIMEN DETERIORATED BY ALKALI-SILICA REACTION (ASR)

Yukio Hiroi[1*], Takashi Yamamoto[2], Yoshihiko Toda[3], Hideki Manabe[4], Toyo Miyagawa[5]

[1]Engineering Department, PC Division, IHI Construction Service Co., Ltd., Osaka, <u>JAPAN</u>

[2]Department of Civil & Earth Resources Engineering, Kyoto University, Kyoto, <u>JAPAN</u>

[3]Research Institute of System Technology, JIP Techno Science Corporation, Osaka, <u>JAPAN</u>

[4]CORE Institute of Technology Corporation, Osaka, <u>JAPAN</u>

[5]Infra-System Management Research Unit, Kyoto University, Kyoto, <u>JAPAN</u>

**Abstract**

It is critically important to properly and quantitatively evaluate mechanical performance of ASR-affected structures. However, there are no established methods for proper estimation of load carrying performance of ASR-affected structures because it is extremely difficult to determine the degree of three-dimensional deterioration by ASR. In this study real-scale large prestressed concrete (PC) beam specimens were exposed to 7.5 years of ASR deterioration for long-term measurement and subjected to flexural loading test. Core samples were taken from the specimens after the loading test for mechanical property tests on ASR-affected concrete. The authors carried out nonlinear FE analysis using the measured mechanical property values in an attempt to reproduce the loading test. This report discusses the mechanical property values of the concrete core samples, analysis techniques and a comparison between the analysis and the experiment.

**Keywords**: post-tensioned prestressed concrete beam, static loading test, analytical method, flexural behavior, mechanical properties of drilled cores

## 1    INTRODUCTION

Deterioration by alkali-silica reaction (ASR) in civil infrastructures has been reported from many places in Japan [1], and there still seem to be more structures left without being recognized to have the ASR problem. One of the reasons for this situation is that high-level knowledge and expertise are required to make accurate diagnosis of ASR, perform analytical evaluation of load carrying performance or select proper preventive or corrective measures. Efforts have been poured into the research of ASR, and important findings have been obtained on various themes such as materials science of rocks and minerals as concrete aggregate [2], expansion behavior and mechanical performance of concrete [3] and fracture mechanism of steel reinforcement [1]. The research focus has been also placed on load carrying performance of ASR-affected structures [4]. However, most of such studies are experimental ones using specimens of ordinary sizes. Very few reports are available on load carrying performance of a real-scale prestressed concrete (PC) beam structure.

The lack of proper methods for evaluating present-time load carrying performance of ASR-affected structures inevitably leads to use of estimates and assumptions in the strengthening design. As a result, unnecessary or over-designed measures can be taken, or serious deterioration which may affect safety can be overlooked. Therefore, it is urgently needed to establish a method that provides good estimation of load carrying performance of ASR-affected structures.

The purpose of this study is to establish a load carrying performance estimation method for ASR-affected PC beam structures. The study consists of the followings: (1) long-term measurement using specimens to determine the degree of ASR deterioration; (2) loading test to determine load carrying performance of the ASR-affected specimen; (3) mechanical property evaluation using the core samples taken from the ASR-affected specimen; and (4) examination of an analytical evaluation method using nonlinear FE analysis for load carrying performance of ASR-affected PC beam

---

*Correspondence to: yukio_hiroi@iik.ihi.co.jp

structures. The results demonstrated that the proposed method was basically capable of providing estimation of initial stiffness, maximum load and strains of ASR-affected PC beams. This paper reports the details of (3) and (4) described above.

## 2    SPECIMENS AND LOADING TEST RESULTS
### 2.1    Outline of the specimens
Four post-tensioned PC beam specimens simulating real PC structures were prepared [5] and exposed to 7.5 years of ASR deterioration for long-term measurement. The ASR and control specimens had the same specifications, except for the aggregate used: reactive aggregate in the ASR specimens; and non-reactive aggregate in the control specimens. Each type was prepared in two sizes: large and medium. Figure 1 shows the shape and dimensions of the large specimens. The report in the following sections is about the large-sized ASR and control specimens.

### 2.2    Loading test results
Four-point bending test was carried out on each specimen. Both large specimens were found to fail in bending. Flexural cracks occurred in the bottom surface in the uniform moment region and developed, and final load was reached when the concrete failed by crushing at the extreme compression fiber after yielding of the prestressing bars. Final loads were at similar levels: 4885 kN in the ASR specimen; and 4908 kN in the control specimen. Figure 2 shows the load-displacement curves of the specimens. Further details of the loading test results are provided in the other paper from the same study [6].

## 3    MECHANICAL PROPERTY EVALUATION USING THE CONCRETE CORES SAMPLED FROM THE ASR-AFFECTED SPECIMEN
### 3.1    Coring locations
Concrete core test pieces (TPs) were sampled from the specimens after the loading test, and their mechanical properties [compressive strength ($f_c$), static elastic modulus ($E_c$) and tensile strength ($f_t$)] were measured. The samples were taken both vertically and longitudinally as shown in Figure 3. The longitudinal cores which were in the direction of prestress were taken from both the inside [$a$ in Figure 3] and the surface [$b$ in Figure 3] to take into account variations in the degree of deterioration.

### 3.2    Mechanical properties of the core samples
Figure 4 shows the mechanical property measurement results of the TPs taken from the large specimens. The ratio of the value of the ASR specimen to that of the control specimen (ASR/control ratio) of $f_c$ was 68% for the inside longitudinal TPs, 59% for the surface longitudinal TPs and 45% for the vertical TPs. The ASR/control ratio of $E_c$ was 61% for the inside longitudinal TPs, 53% for the surface longitudinal TPs and 18% for the vertical TPs, showing more significant decreases as compared to $f_c$. The relationship between $f_c$ and $E_c/f_c$ (Figure 5) [7] showed that $E_c/f_c$ of the longitudinal TPs of the ASR specimen remained at similar levels to those of the control specimen irrespective of the decrease in $f_c$, whereas that of the vertical TPs decreased significantly with the decrease in $f_c$. This was likely caused by two reasons. One was the absence of confinement effect of prestress or other forces. The other was the ASR cracks prominent in the longitudinal direction of the beam which were perpendicular to the compressive load in the vertical TPs (Figure 6). Deformation by compression would have increased as these cracks closed under the compressive load, possibly leading to significant decreases in the mechanical property values, especially in $E_c$. The ASR/control ratio of $f_t$ was about 50% in both longitudinal and vertical TPs.

## 4    ANALYTICAL EVALUATION METHOD FOR LOAD CARRYING PERFORMANCE OF ASR-AFFECTED PC BEAMS
### 4.1    Outline of the analytical evaluation method
In order to establish a load carrying performance evaluation method applicable to real structures affected by ASR, the authors examined an analytical method using a general-purpose three-dimensional nonlinear FEA software (DIANA 9.4.4, TNO DIANA BV), with input values taken from practically available information, i.e., concrete mechanical property values estimated from the cracks observed in the surface of members or the amount of expansion, or those estimated from the values of core samples.

## 4.2 Analysis conditions

*Analysis model and method*

Figure 7 shows the model used for the FE analysis. Concrete was expressed with solid elements, and prestressing and reinforcing bars were expressed with embedded steel reinforcement elements. Self-weight and prestress were considered as the initial conditions, and displacement-controlled analysis was carried out by applying incremental forced displacement to the loading point.

*Analysis conditions*

Compressive stress-strain relationship in concrete was expressed with a quadratic curve model combined with linear compression softening [8], and tensile stress-strain relationship in concrete was expressed with a model consisting of linear elasticity up to the tensile strength and linear softening after initiation of cracks (Figure 8). A smeared crack model with fixed crack angles was used. The concept of fracture energy was introduced in the softening region after the peak in the stress-strain curves by using the following equations for both the control and ASR specimens. Compressive fracture energy $G_{fc}$ (in N/mm) was calculated by using Equation (1) based on the study by Yamaya et al. [9], and tensile fracture energy $G_{ft}$ (in N/mm) was calculated by using Equation (2) based on the Standard Specifications for Concrete Structures [10]:

$$G_{fc} = 8.77 \times fc^{1/2} \qquad (1)$$
$$G_{ft} = d_{max}^{1/3} \times fc^{1/3}/100 \qquad (2)$$

where, $fc$: compressive strength (in N/mm²); and $d_{max}$: maximum size of coarse aggregate (in mm).

Stress-strain relationship in the reinforcing bars was expressed with a bilinear model, and that in the prestressing bars was expressed with a trilinear model.

## 4.3 Results with the control specimen

Table 1 shows the concrete mechanical property values used for the control specimen in the analysis, and Figure 9 shows the load-displacement curves for the control specimen obtained by the analysis. The analysis results for the control specimen were mostly consistent with the loading test results including initial stiffness and maximum load. This demonstrated the validity of the analysis model and method used.

## 4.4 Analysis inputs for the ASR specimen

Table 2 shows the measured mechanical property values of the TPs of the ASR and control specimens. The values of the ASR specimen TPs were used in the analysis as the inputs for the surface region of the ASR specimen, because the measurement results were considered to well represent the condition of the surface region which was not subjected to confinement (Figure 10). The specimens were cut vertically after the loading test, and the cut surfaces were inspected. Visible ASR cracks were found only in the surface region, suggesting that the degree of deterioration was smaller in the inside than in the surface. Using the expansion values measured at the mid-span cross section, the authors made an estimation based on the relationship between the mechanical property values and expansion shown in Figure 11 [1,11]. Table 3 shows the estimation results. It is known that longitudinal cracks appear in the surface of an ASR-affected PC structure. Such cracks are considered to be present also in the inside as micro-cracks. The TPs taken from the ASR specimen showed a decrease in compressive strength. On the other hand, the loading test results showed no decrease in maximum load despite the decrease in initial stiffness. These findings allow an assumption that, as long as micro-cracks remain within the inside region, mechanical property values are similar to those in sound state, with expansion rate in the longitudinal direction being zero. However, according to Sekimoto et al. [12], mechanical property values can be reduced despite the confinement by the reinforcing bars on ASR expansion, with an especially significant decrease in static elastic modulus. Although anisotropic data were obtained by estimation as shown in Table 3, only longitudinal data were selected for the analysis due to the assumption that bending would prevail in the specimens in the current study, as well as in order to assess reproducibility using the isotropic data with respect to the loading test results. The mechanical property values of the ASR specimen were expressed in ratios to those of the control specimen.

Sensitivity analysis was carried out to determine the influence of the inside mechanical property values on the bending load carrying performance of the ASR specimen. The ASR/control

ratio of $f_c$ was changed between 70%, 80% and 90%, and that of $E_c$ was changed between 60% and 80%. These ratios were selected by referring to those of the inside TPs by measurement ($f_c$ = 68%, $E_c$ = 61%). The measured longitudinal TP values ($f_c$ = 63%, $E_c$ = 58% and $f_t$ = 45%) were used for the surface mechanical property inputs. The analysis results showed that maximum load increased only gradually with the increase of $f_c$, indicating only minor influence of inside $f_c$ on maximum load. In contrast, inside $E_c$ was found to have an influence on initial stiffness, yielding the best fit with the loading test results at 80%. Based on these results, the property values were differentiated between the surface and the inside regions defined in Figure 10 (surface-inside separate property setting), with the inside $f_c$ and $E_c$ being set to 90% and 80%, respectively, to the control as shown in Table 4.

The strain in the prestressing bars measured during the loading test shown in Table 2 was used as the prestress in the ASR specimen. This value takes into account the increase of about 10% by the longitudinal expansion due to ASR.

### 4.5    Analysis results for the ASR specimen
*Maximum load and displacement*

Figure 12 shows the load-displacement relationship in the ASR specimen by the analysis. Like those observed in the control specimen, flexural cracks in the ASR specimen developed from the bottom surface of the specimen, and the load started to decrease due to compressive softening at the extreme compression fiber in the uniform moment region. Failure mode by the analysis was same as the experiment results. The analysis results of the control specimen (Figure 9) were mostly consistent with the loading test results including initial stiffness and maximum load. In contrast, although initial stiffness of the ASR specimen by the analysis was consistent with the loading test results, maximum load was slightly lower than that by the loading test (94% to the experiment value). Stiffness after initiation of flexural cracks was found to be different from the loading test results.

*Strains*

Longitudinal strain in the concrete at the extreme compression fiber of the ASR specimen shown in Figure 12 was in good fit with the loading test results. This suggests that although the longitudinal ASR cracks occurred in the surface of the specimen, the concrete of the top surface at the extreme compression fiber would have behaved as one element, without making discontinuous behaviors. Strain in the bottom prestressing bar was also found to be mostly consistent with the loading test results.

### 4.6    Discussion about the analytical evaluation method

Behavior of the ASR specimen during the loading test was generally successfully reproduced by the analytical evaluation method described above. However, difference was found in stiffness after initiation of flexural cracks between the analysis and the experiment. During the loading test upward development of flexural cracks in the ASR specimen was found to be slow due to the horizontal ASR cracks, slowing the decrease in stiffness after initiation of cracks [13]. This characteristic behavior of flexural cracks is not considered in the analysis model in the current study, which is likely the cause of the difference in stiffness observed after the crack initiation.

These findings demonstrated that it would be generally possible to estimate initial stiffness, maximum load and strains of an ASR-affected PC beam structure like the current specimens in which bending would prevail, by using the proposed method which consisted of determination of the physical properties of the core samples taken from the specimens, estimation of mechanical property values of ASR-affected concrete from the core data, and FE analysis using a model with different property settings between the surface and the inside based on the estimation.

The proposed evaluation method uses the mechanical property values estimated from the test results on the core samples or expansion measurement. It must be difficult practically to obtain these analysis inputs from actual ASR-affected PC structures in service. The next research focus is to determine the relationship of crack density or other surface deterioration indices with mechanical property retention rates and apply it to obtaining analysis inputs.

## 5    CONCLUSIONS

This study investigated an analytical evaluation method for estimation of bending load carrying performance of ASR-affected post-tensioned PC beam structures, and demonstrated that the proposed method was generally capable of reproducing the loading test results. The findings are summarized below.

- Measurement on core samples after the loading test showed that property values decreased even in the longitudinal cores in which confinement was present. The decrease behavior was

more significant in static elastic modulus and tensile strength than in compressive strength, and the decrease rate was larger in the vertical cores in which confinement was absent.

- The authors proposed an analytical evaluation method for estimating load carrying performance of ASR-affected PC beam structures. The method uses a general-purpose three-dimensional nonlinear FEA software and applies the surface-inside separate property setting to the analysis model to differentiate the mechanical property values between the surface and the inside across the vertical cross-section. It was demonstrated that the proposed method was generally capable of reproducing the loading test results in initial stiffness, maximum load and strains of the ASR specimen.

- It was found that influence of compressive strength of the inside concrete on maximum load was only minor, whereas static elastic modulus of the inside concrete had influence on initial stiffness.

## 6    REFERENCES

[1]    Japan Society of Civil Engineers (2005): State-of-the-art report on the countermeasures for damage due to alkali-silica reaction – Rupture of reinforcing bars. Concrete Library (124). (in Japanese).

[2]    Japan Concrete Institute (2008): Technical Committee Reports 2008-Digest Edition (JCI-TC062A: Technical Committee on ASR Inhibition Measures and Diagnosis Based on its Action Mechanisms).

[3]    Kubo, Y, Ueda, T, Kuroda, T, and Nomura, N (2006): Influence of ASR expansion on mechanical properties of concrete. Proceedings of the Japan Concrete Institute (28.1): 1691-1696. (in Japanese).

[4]    Ueda, N, Nakamura, H, Kunieda, M, Maeno, H, Morishita, N, and Asai, H (2011): Evaluations on ASR damage of concrete structure and its structural performance. Journal of JSCE, E2 (67.1): 28-47. (in Japanese).

[5]    Hiroi, Y, Manabe, H, Ihaya, T, Ookubo, T, and Miyagawa, T (2008): Experimental study on the long-term properties of prestressed concrete members affected by alkali-silica reaction (ASR). 13th ICAAR 2008 Proceedings: 754-763.

[6]    Yokoyama, T, Miyagawa, T, Yamamoto, T, Manabe, H, Ookubo, T, and Hiroi, Y (to be printed): Long-term deterioration of quasi-actual scale prestressed concrete beam due to alkali-silica reaction. 15th ICAAR Proceedings, July 3-7, 2016, São Paulo, Brazil.

[7]    Kobayashi, K, Mori, Y, and Nomura, K (1993): Method of diagnosing alkali-silica reaction by compressive loading test. Journal of JSCE (18.460): 151-154. (in Japanese).

[8]    Japan Concrete Institute (2008): Basics, Applications and Practices of Nonlinear Finite Element Methods for Structural Engineers. (in Japanese).

[9]    Yamaya, A, Nakamura, H, and Higai, T (1999): Shear behavior analyses of RC beams using rotating crack model. Journal of JSCE (43.620): 187-199. (in Japanese).

[10]    Japan Society of Civil Engineers Concrete Committee (2013): Standard Specifications for Concrete Structures: Design. (in Japanese; 2007 in English).

[11]    Clark, LA (1989): Critical review of the structural implication of the alkali-silica reaction in concrete. Transport and Road Research Laboratory Contractor Report (169).

[12]    Sekimoto, H, Shimizu, H, Watanabe, Y, and Ishikawa, T (2005): Study of properties for strength evaluation of turbine generator foundation affected by alkali-silica reaction. Proceedings of the Japan Concrete Institute. (27.2): 1555-1560. (in Japanese).

[13]    Tada, Y, Sato, T, Yamamoto, T, and Hiroi, Y (2014): Study of FEA models for load carrying performance evaluation on PC beam specimens affected by ASR. Japan Prestressed Concrete Engineering Association Proceedings of the 23rd Symposium on Developments in Prestressed Concrete: 95-100. (in Japanese).

TABLE 1: Concrete mechanical property values used for the control specimen in the analysis.

| Static elastic modulus (N/mm²) | Compressive strength (N/mm²) | Tensile strength (N/mm²) |
|---|---|---|
| 34,100 | 61.3 | 3.56 |

TABLE 2: Measured mechanical property values of the TPs.

| | | Control | ASR | ASR/control |
|---|---|---|---|---|
| $f_c$ (N/mm²) | Total average | 61.3 | 34.9 | 0.57 |
| | Longitudinal average | 61.6 | 38.9 | 0.63 |
| | Vertical average | 60.8 | 27.0 | 0.44 |
| $E_c$ (N/mm²) | Total average | 34100 | 15100 | 0.44 |
| | Longitudinal average | 34400 | 19650 | 0.57 |
| | Vertical average | 33500 | 6100 | 0.18 |
| $f_t$ (N/mm²) | Total average | 3.56 | 1.66 | 0.47 |
| | Longitudinal average | 3.46 | 1.59 | 0.46 |
| | Vertical average | 3.75 | 1.81 | 0.48 |
| Stress in the prestressing bars (N/mm²) | | 631 | 691 | 1.10 |

TABLE 3: Estimated mechanical property values based on the expansion rate.

| | Control | ASR | | |
|---|---|---|---|---|
| | | Longitudinal | Transverse | Vertical |
| Expansion amount (μm) | 0 | 0 | 6500 | 3500 |
| Compressive strength (ASR/control, %) | 100 | 100 | 70 | 70 |
| Elastic modulus (ASR/control, %) | 100 | 100 | 33 | 44 |
| Tensile strength (ASR/control, %) | 100 | 100 | 42 | 54 |

TABLE 4: Concrete mechanical property values used for the ASR specimen in the analysis.

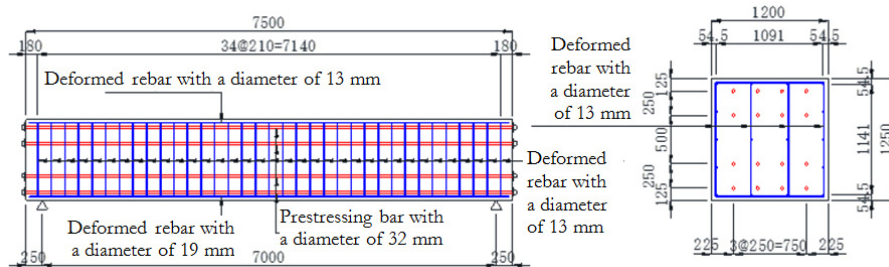| | Control (kN) | ASR | | | |
|---|---|---|---|---|---|
| | | Surface (kN) | Surface/control (%) | Inside (kN) | Inside/control (%) |
| $f_c$ | 61.3 | 38.9 | 63 | 55.2 | 90 |
| $E_c$ | 34100 | 19650 | 58 | 27280 | 80 |
| $f_t$ | 3.56 | 1.59 | 45 | 3.2 | 90 |



FIGURE 1: Configuration of the large specimens
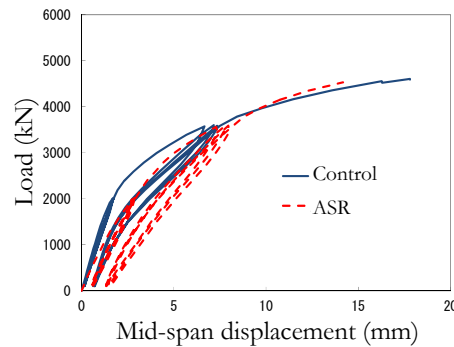


FIGURE 2: Load-displacement curves of the large specimens

↓: Cut with a wire saw.    Core size: 100 mm in diameter, 250 mm in length

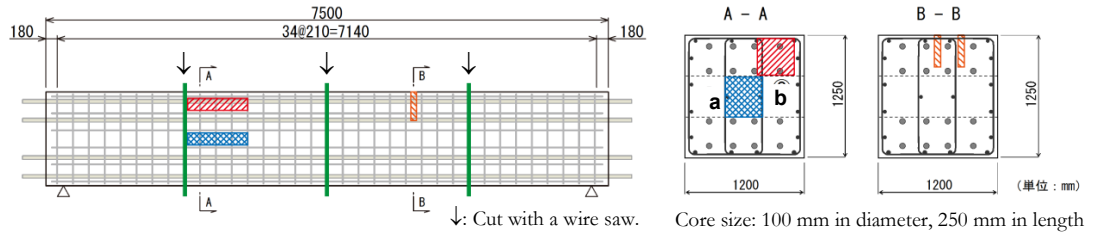FIGURE 3: Test piece sampling locations
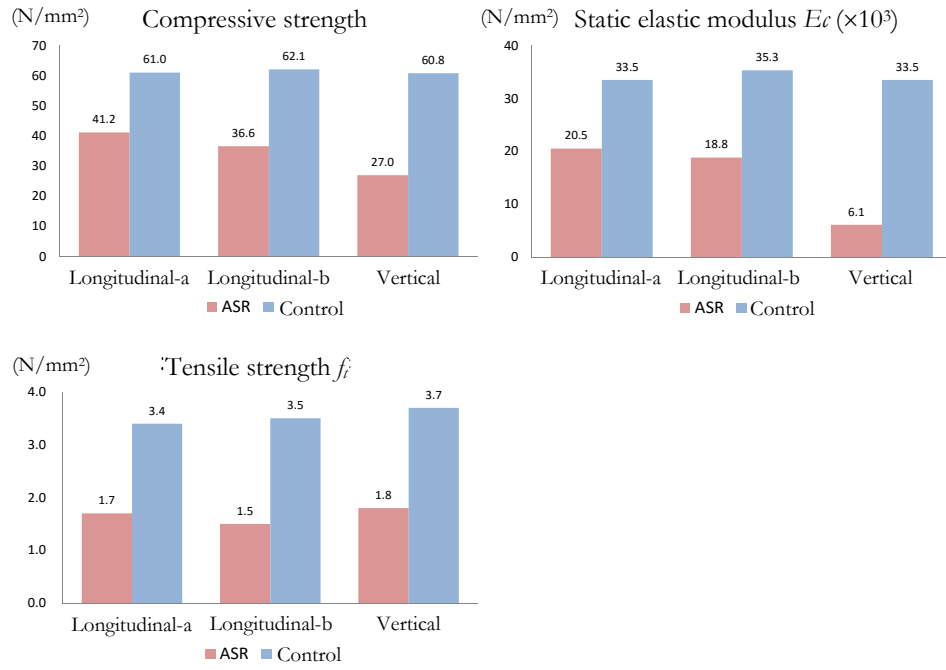


FIGURE 4: Measured mechanical property values of the test pieces from the large specimens



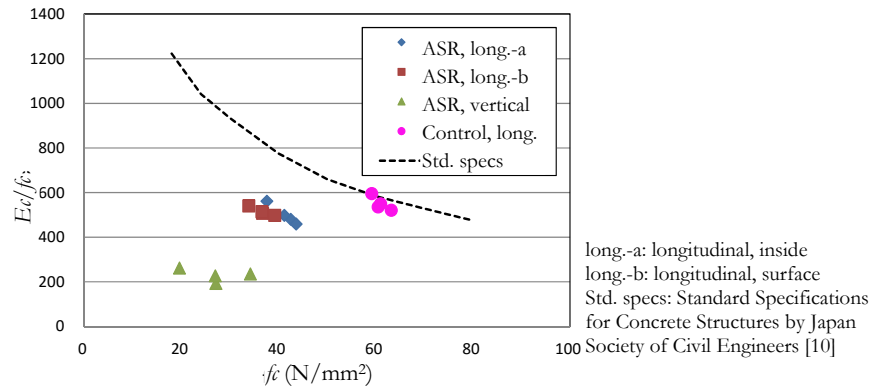long.-a: longitudinal, inside
long.-b: longitudinal, surface
Std. specs: Standard Specifications
for Concrete Structures by Japan
Society of Civil Engineers [10]

FIGURE 5: Relationship between $f_c$ and $E_c/f_c$ in the test pieces [7]
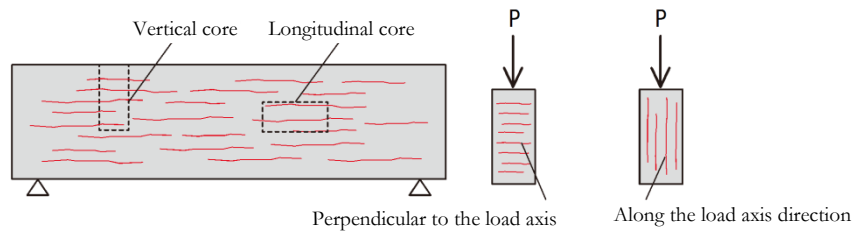
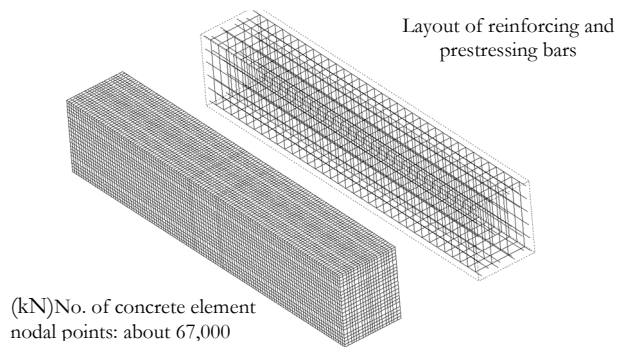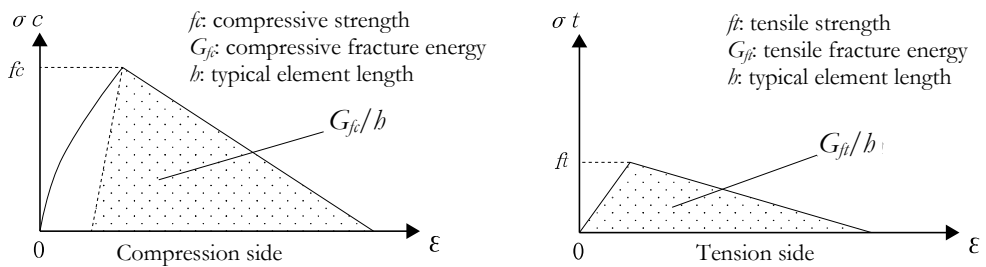FIGURE 6: Relationship between the core samples and horizontal cracks

Vertical core    Longitudinal core

P    P

Perpendicular to the load axis    Along the load axis direction



Layout of reinforcing and prestressing bars

(kN)No. of concrete element nodal points: about 67,000

FIGURE 7: FEA model



$\sigma c$

$fc$

$G_{fc}/h$

0    Compression side    $\varepsilon$

$fc$: compressive strength
$G_{fc}$: compressive fracture energy
$h$: typical element length

$\sigma t$

$ft$

$G_{ft}/h$

0    Tension side    $\varepsilon$

$ft$: tensile strength
$G_{ft}$: tensile fracture energy
$h$: typical element length

FIGURE 8: Stress-strain



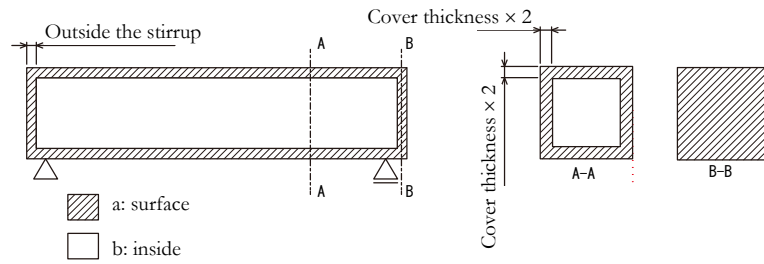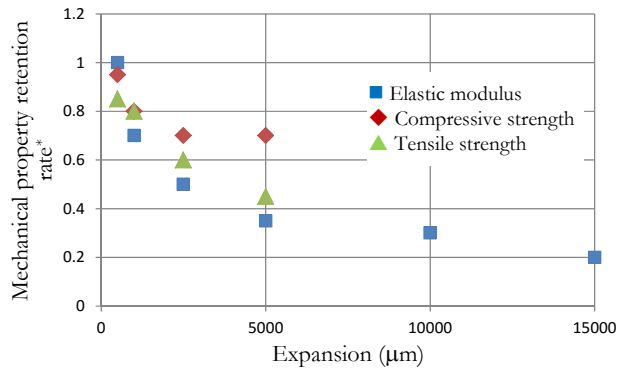FIGURE 9: Load-displacement curves by the analysis for the large control specimen

FIGURE 10: Definition of the surface and inside regions



*Ratio of the value of an ASR-affected sample to that of control
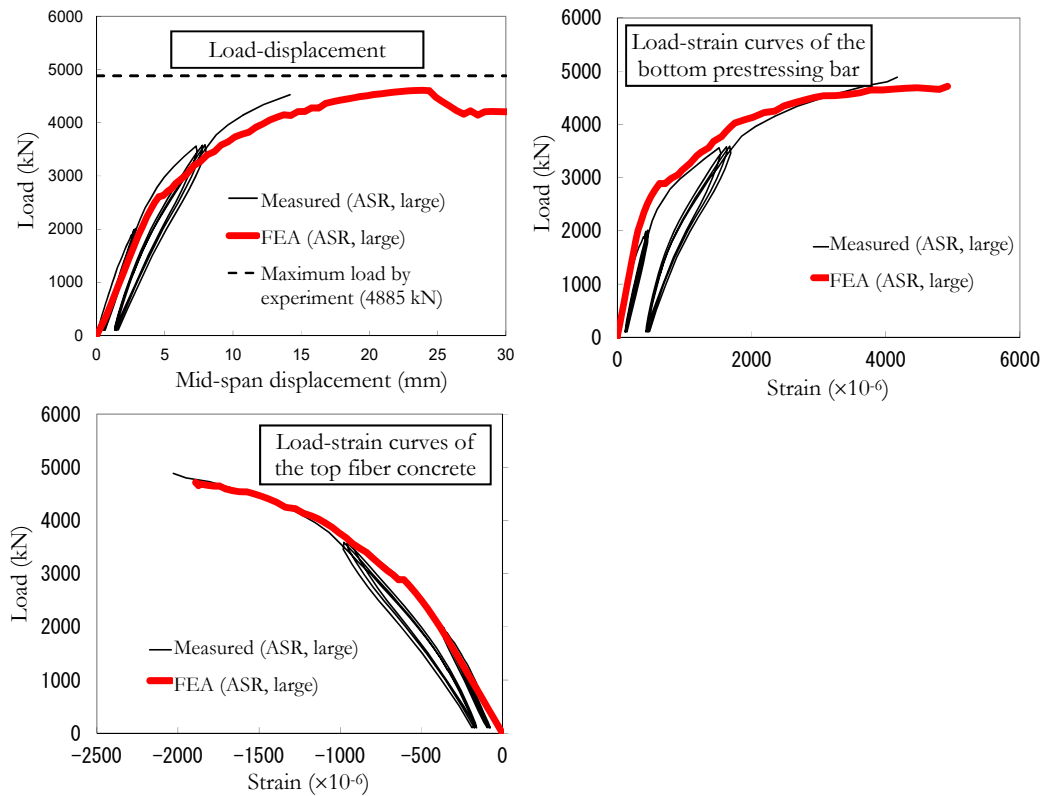
FIGURE 11: Mechanical property retention rates vs. expansion [1,11]



FIGURE 12: Analysis results for the large ASR specimen